Received: 27 March 2023 | Revised: 5 June 2023 | Accepted: 20 June 2023

DOI: 10.1002/syn.22280

SHORT COMMUNICATION

SYNAPSE WILEY

Autoradiographic characterization of [^{18}F]PSMA-1007 binding in rat brain

Majken B. Thomsen[1,2] | Anne M. Landau[1,2] | Dirk Bender[2] | Paul Cumming[3,4]

[1]Translational Neuropsychiatry Unit, Department of Clinical Medicine, Aarhus University, Aarhus, Denmark

[2]Department of Nuclear Medicine and PET, Department of Clinical Medicine, Aarhus University, Aarhus, Denmark

[3]Department of Nuclear Medicine, Bern University Hospital, Bern, Switzerland

[4]School of Psychology and Counselling, Queensland University of Technology, Brisbane, Australia

Correspondence
Majken Thomsen, Translational Neuropsychiatry Unit, Aarhus University Hospital, A601, Palle Juul-Jensen Boulevard 99, 8200 Aarhus N, Denmark.
Email: majken.thomsen@clin.au.dk

Funding information
Parkinsonforeningen;
Independent Research Fund Denmark

Abstract

Carboxypeptidase II (CBPII) in brain metabolizes the neuroactive substance N-acetyl-*L*-aspartyl-*L*-glutamate (NAGG) to yield the elements of glutamate and N-acetyl-aspartate (NAA). In peripheral organs, CBPII is known as prostrate specific membrane antigen (PSMA), which presents an important target for nuclear medicine imaging in prostate cancer. Available PSMA ligands for PET imaging do not cross the blood–brain barrier, and there is scant knowledge of the neurobiology of CBPII, despite its implication in the regulation of glutamatergic neurotransmission. In this study we used the clinical PET tracer [^{18}F]-PSMA-1007 ([^{18}F]PSMA) for an autoradiographic characterization of CGPII in rat brain. Ligand binding and displacement curves indicated a single site in brain, with K_D of about 0.5 nM, and B_{max} ranging from 9 nM in cortex to 19 nM in white matter (corpus callosum and fimbria) and 24 nM in hypothalamus. The binding properties of [^{18}F]PSMA in vitro should enable its use for autoradiographic investigations of CBPII expression in animal models of human neuropsychiatric conditions.

KEYWORDS
autoradiography, brain, carboxypeptidase II, [^{18}F]-PSMA-1007, PSMA

1 | INTRODUCTION

The discovery of radioligands for prostate specific membrane antigen (PSMA) has revolutionized the assessment and treatment of prostate cancer. The PSMA binding site is located on the enzyme glutamate carboxypeptidase II (GCPII), also known as N-acetyl-L-aspartyl-*L*-glutamate peptidase I (Carter et al., 1996), which is encoded by the *FOLH1* (folate hydrolase 1) gene. This enzyme has aberrantly high expression in the plasma membrane of prostatic cancer cells, which affords high tumor to background contrast in positron emission tomography (PET) studies with its prototype urea-based ligand [^{68}Ga]-PSMA-11 and its structural congeners, including [^{18}F]PSMA-1007 ([^{18}F]PSMA; Awenat et al., 2021). The brain also possesses a high activity of GCPII, where it catalyzes the hydrolysis of N-acetyl-*L*-aspartyl-*L*-glutamate (NAAG) to glutamate and N-acetyl-*L*-aspartate (NAA). However, available radioligands for GCPII obtain scant penetration across the blood–brain barrier (BBB); the brain appears as a void in clinical imaging, although application of focused ultrasound enables tracer uptake in brain of living rats (Airan et al., 2017).

In seemingly the only study of its type, quantitative autoradiography with the [^{125}I]-labeled GCPII antagonist *N*-[*N*-[(*S*)−1,3-dicarboxypropyl]carbamoyl]-*S*-3-iodo-*L*-tyrosine ([^{125}I]-DCIT) revealed abundant binding in rat brain cryostat sections, with a complex distribution pattern (Guilarte et al., 2005). However, that study entailed a single radioligand concentration of 5 nM, which could not afford quantitation of

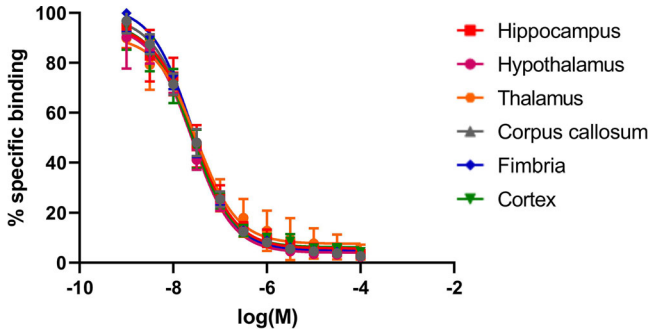

FIGURE 1 The displacement [^{18}F]-PSMA binding (2 nM) in six regions of rat brain as a function of increasing concentration of the glutamate carboxypeptidase II blocker 2-PMPA (0–100 μM) shows the % specific binding with SD.

saturation binding parameters. Furthermore, genetic deletion studies of GCPII in mice indicated a second peptidase activity with 100-fold lower affinity for the antagonist 2-(phosphonomethyl)pentanedioic acid (2-PMPA) (Bacich et al., 2002). It remains unknown if the [^{125}I]-DCIT binding study indicates a unitary GCPII binding site, or a mixture of two different binding components. In order to establish further the distribution of GCPII binding sites in rat brain, we undertook a series of quantitative autoradiographic studies using [^{18}F]-PSMA, an emerging PET tracer for detection of metastatic prostate cancer. To this end, we first undertook a displacement series with the GCPII inhibitor 2-PMPA to test the hypothesis that only one binding site is present in rat brain, and then proceeded to undertake saturation binding studies with [^{18}F]-PSMA, so as to establish B_{max}, the abundance of the enzyme in representative brain regions.

2 | METHODS

Female Sprague-Dawley rats (n = 5; weight ~250 g; Taconic Biosciences) were deeply anesthetized for brain removal, followed by immersion in isopentane (−40°C) and storage (−80°C). We mounted brains in a cryostat (CryoStar NX70, Thermo Fischer) at – 20°C and cut coronal sections 20 μm thick at the level of thalamus, which were thaw-mounted on polysine-coated slides (Epredia). After air-drying, the slides were stored at −80°C until use. [^{18}F]-PSMA was prepared at the cyclotron radiochemistry facility according to established methods (Cardinale et al., 2017a), yielding a formulation containing the radioligand at a mean concentration of 1.2 μM (range: 0.22–2.8) at the time of delivery, with mean initial molar activity of 2335 GBq/μmol (range: 377–5155), thus less than 3% of the theoretical molar activity of cyclotron-generated fluorine-18. After brief preincubation in buffer (50 mM HEPES, 0.9% NaCl, pH 7.5), 1 mL portions of [^{18}F]-PSMA solution were placed on the slides, which were contained in a plexiglass box equipped with a spirit level. Since most of the radioligand solution consists of [^{19}F]-PSMA and only a small fraction is [^{18}F]-PSMA, the decay of [^{18}F]-PSMA does not change the overall ligand concentration. After incubation for 45 min at room temperature, slides were washed three times in ice-cold HEPES buffer for 1 min each time; following removal of buffer, slides were dried under a cold air stream. We exposed the dried slides to an imaging screen (Fujifilm MS 2025) for 60 min, and quantified the exposure using a Typhoon imaging reader (Amersham) in conjunction with ImageQuantTL analysis software.

In the initial displacement studies, the [^{18}F]-PSMA concentration was 2 nM, in the presence of 2-(phosphonomethyl)pentanedioic acid (2-PMPA, Sigma) at the following range of final concentrations: 0, 0.001, 0.0032, 0.01, 0.032, 0.1, 0.32, 1, 3.2, 10, 32, and 100 μM. At each competitor concentration, we measured the binding density in the following brain regions: hippocampus, corpus callosum, cortex, fimbria, thalamus, and hypothalamus. We obtained quantitation relative to dried spots (on TLC Silaíca Gel slides, Sigma-Aldrich) of known radioligand concentration. To estimate the saturation binding parameters, we next undertook incubations in which the final [^{18}F]-PSMA concentrations were 0.1, 0.3, 1, 3, and 10 nM, with nonspecific binding measured in the presence of 2-PMPA (10 μM). We fitted a one- and two-site models to the saturation series using GraphPad Prism (v9.4.1), and calculated the regional B_{max} and K_D values in three independent replications.

3 | RESULTS

Comparison of the one- and two-site model fit of the saturation curve using the Akaike's information criterion (AIC) revealed that the one-site model was the best fit (>96% chance as compared to the two-site model) in all examined brain regions. Figure 1 shows the displacement of a fixed concentration of [^{18}F]-PSMA (2 nM) by increasing concentrations of 2-PMPA (0–100 μM); fitting of the one-site model to the curves revealed nearly identical K_i values for the six brain regions (Table 1). [^{18}F]-PSMA autoradiography (Figures 2 and 3 and Table 1) showed lowest binding in the cortex and hippocampus, intermediate binding in white matter (corpus callosum and fimbria) and thalamus, and highest binding in

TABLE 1 The magnitude of K_i for the inhibitor 2-PMPA against [^{18}F]-PSMA (2 nM) and the saturation binding parameters K_D and B_{max} for [^{18}F]-PSMA binding in six brain regions.

	Corpus callosum	Fimbria	Hippocampus	Neocortex	Thalamus	Hypothalamus
K_i (nM)	4.59 ± 1.07	5.43 ± 1.09	4.93 ± 1.14	3.49 ± 1.13	6.19 ± 1.18	5.15 ± 1.12
K_D (nM)	0.41 ± 0.23	0.54 ± 0.16	0.42 ± 0.12	0.33 ± 0.10	0.48 ± 0.09	0.51 ± 0.12
B_{max} (nM)	18.9 ± 2.28	19.4 ± 1.38	10.2 ± 0.67	9.08 ± 0.57	20.0 ± 0.91	23.9 ± 1.32

Note: Each value is the mean (± SE) of three separate determinations.

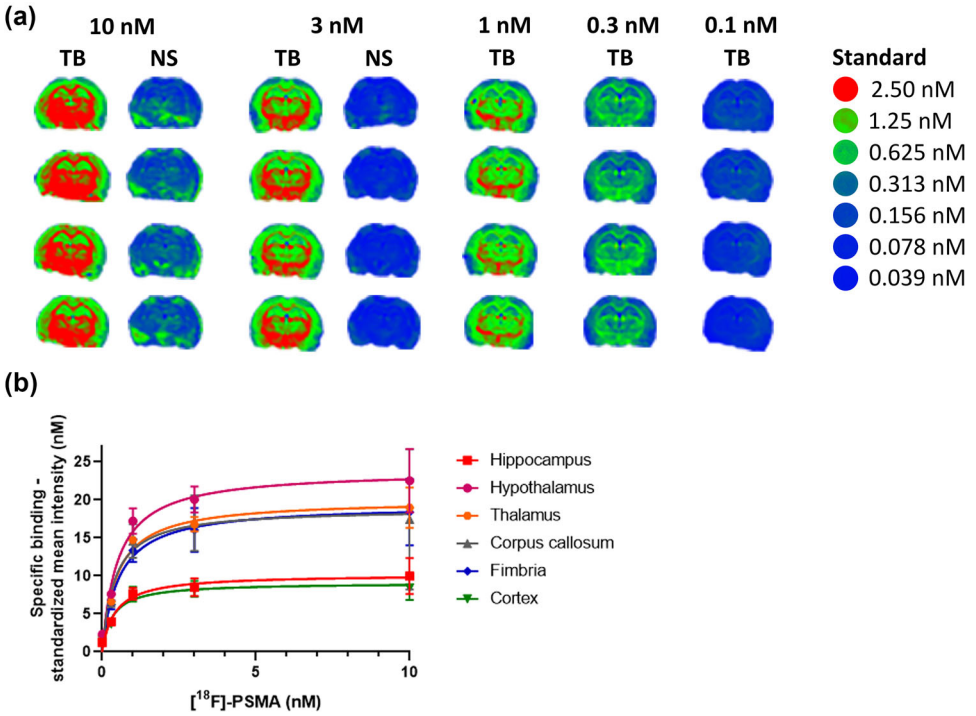

FIGURE 2 In vitro autoradiography of [^{18}F]-PSMA in coronal rat brain sections (A). Nonspecific binding was determined in the presence of 2-PMPA (10 μM). TB: total binding, NS: nonspecific binding. Saturation binding curve (B) shows the specific binding with SD at five [^{18}F]-PSMA concentrations (0.1–10 nM) in six representative brain regions.

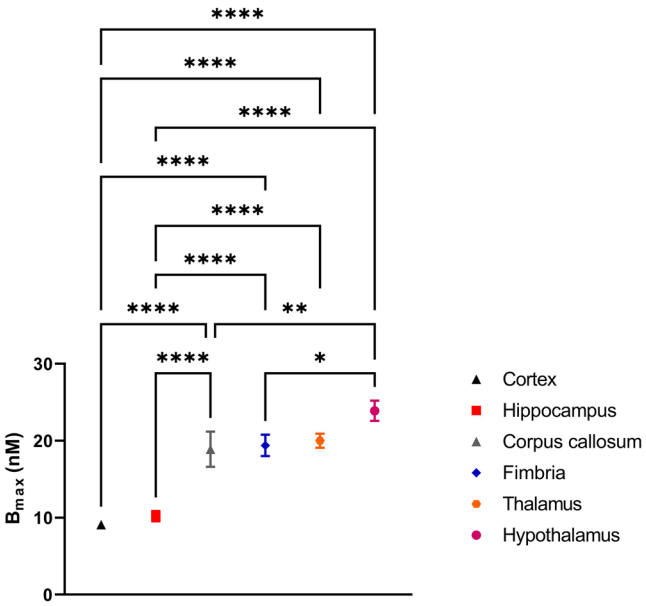

FIGURE 3 In vitro autoradiography B_{max} (nM) values with SD of [^{18}F]-PSMA binding in coronal rat brain sections. *$p < .05$, **$p < .01$, ****$p < .0001$.

the hypothalamus. One-way ANOVA comparison of B_{max} of the 6 brain regions shows significant differences between regions ($p < .0001$). Sidak's multiple comparison show no significant difference between cortex and hippocampus ($p = .999$), while both regions had significantly lower B_{max} than the four remaining regions ($p < .0001$). Similarly, B_{max} was significantly higher in hypothalamus than corpus callosum ($p < .01$), fimbria ($p < .05$), cortex, and hippocampus (both $p < .0001$), but not thalamus ($p = .52$).

In the 2-PMPA displacement study against 2 nM [^{18}F]-PSMA, the K_i was in the range of 3.5–6.2 nM (Table 1). In the saturation binding study, [^{18}F]-PSMA had K_D ranging from 0.3 to 0.5 nM by and B_{max} ranging from 9 to 24 nM by region (Table 1). The nonspecific binding of [^{18}F]-PSMA (10 nM) was less than 10% of the total binding, thus indicating a favorable signal-to-background ratio of quantitative autoradiography.

4 | DISCUSSION

MR spectroscopy showed NAAG concentrations of about 1 mM in gray matter versus 2 mM in white matter of human brain, whereas the NAA concentration was uniformly 8 mM (Pouwels & Frahm, 1997). Indeed, NAA is responsible for one of the largest brain signals in the proton MR spectrum, where it serves as a marker for neuronal integrity (Croall et al., 2015). Brain levels of NAAG are maintained by the competing actions of GCPII, which has a 130 nM binding constant for NAAG in vitro (Mesters et al., 2006) and a specific NAAG peptidase. Insofar as NAAG is an agonist at type 3 metabotropic receptors (GluR3) (Wroblewska et al., 1997), NAAG may be the most abundant neurotransmitter in brain, while also serving as an important reservoir for the excitatory neurotransmitter glutamate. As such, the activity of GCPII in brain potentially regulates important aspects of synaptic transmission. The predominant site of GCPII expression is in astroglia, with additional neuronal distribution in neurons, where it has a predominantly presynaptic distribution, consistent with its role as an inhibitory autoreceptor regulating the release of glutamate (Sacha et al., 2007). Given these associations, there is a surprisingly little knowledge about the neurobiology of GCPII in brain. Western blot analysis indicated a heterogeneous distribution of GCPII in human brain, with concentrations in the range 50–300 ng/mg total protein (Sacha et al., 2007). From its molecular weight of 80 kDa, one can thus predict a brain GCPII concentration of about 100 nM.

Results of our displacement and saturation binding studies concur in indicating a single binding site for [^{18}F]-PSMA in rat brain cryostat sections. We identify the specific binding as GCPII, given the displacement with 2-PMPA. These results extend the earlier report on of the GCPII ligand [^{125}I]-DCIT, which showed abundant specific binding in white matter and gray matter in rat brain cryostat sections (Guilarte et al., 2005). The rank order of displaceable [^{125}I]-DCIT binding at the single concentration (5 nM) is in good agreement with the present saturation binding (B_{max}) results for [^{18}F]-PSMA. The present autoradiograms (Figure 2) show ubiquitous distribution of in rat brain, with lowest binding in neocortex, intermediate levels in white matter (corpus callosum and fimbria), and highest binding in hypothalamus. This ubiquity of binding is consistent with a housekeeping role for GCPII in regulating the brain concentrations of NAAG, and its metabolites NAA and glutamate. Furthermore, we note the remarkably high B_{max} values for [^{18}F]-PSMA, which approached 24 nM in hypothalamus (Table 1). These abundances are about fivefold lower than the brain concentration of GCPII estimated from Western blot analysis (Sacha et al., 2007), which likely reflects the profound methodological differences. However, the present B_{max} results are in good agreement with the specific binding of [^{125}I]-DCIT (5 nM), which ranged from 30 to 50 nM in rat brain cryostat sections (Guilarte et al., 2005). The present affinity of [^{18}F]-PSMA for GCPII sites is 10-fold higher than an earlier report for PSMA binding sites in prostate cancer cells (Cardinale et al., 2017b); this discrepancy may call for further investigation of tissue-specific differences in the radioligand binding affinity.

In this study, we diverted [^{18}F]-PSMA from a regular clinical production to application for quantitative autoradiography in rat brain. Relatively few enzymes are amenable for quantitative analysis of B_{max}. The considerable abundance of GCPII binding sites in rat brain is reminiscent of [^{18}F]fluoro-ethylharmol at monoamine oxidase A sites, which had a B_{max} of approximately 600 nM (Maschauer et al., 2015); this high abundance of MAO-A is consistent with its important housekeeping role in regulating the catabolism of biogenic monoamine neurotransmitters such as serotonin and dopamine. As noted above, GCPII in brain may serve as a comparable control point for the regulation of glutamatergic neurotransmission. We find that [^{18}F]-PSMA has binding properties for autoradiography in brain cryostat sections. The spatial blurring of ^{18}F-autoradiography is due to parallax of the emitted positrons, which have an energy of 635 keV. We anticipate that Lutecium-177 PSMA (500 keV beta−) would give comparable results, but Gallium-68 (1.7 mEv beta+) would be worse. Autoradiographic images reported for [^{125}I]-DCIT are clearly superior to present results, but that radioligand is not readily available. As a matter of convenience, small quantities of [^{18}F]-PSMA are divertible from routine clinical productions for use in brain binding studies. Thus, present findings could support the use of [^{18}F]-PSMA for investigations of CBPII expression in studies of animal models of neuropsychiatric disorders and human post mortem studies.

ACKNOWLEDGMENTS

We are thankful to the staff at the Aarhus University Hospital PET Centre and Translational Neuropsychiatry Unit for supporting this work and to the Independent Research Fund Denmark (No. 0134-00226B (AML)) and Parkinsonforeningen (MBT) for providing postdoctoral salary for MBT.

CONFLICT OF INTEREST STATEMENT

The authors declare no conflicts of interest.

DATA AVAILABILITY STATEMENT

The data that support the findings of this study are available from the corresponding author upon reasonable request.

ORCID

Majken B. Thomsen https://orcid.org/0000-0002-2914-9576
Anne M. Landau https://orcid.org/0000-0002-7371-8713

References

Airan, R. D., Foss, C. A., Ellens, N. P., Wang, Y., Mease, R. C., Farahani, K., & Pomper, M. G. (2017). MR-guided delivery of hydrophilic molecular imaging agents across the blood-brain barrier through focused ultrasound. *Molecular Imaging and Biology*, *19*, 24–30.

Awenat, S., Piccardo, A., Carvoeiras, P., Signore, G., Giovanella, L., Prior, J. O., & Treglia, G. (2021). Diagnostic role of (18)F-PSMA-1007 PET/CT in prostate cancer staging: A systematic review. *Diagnostics (Basel)*, 11.

Bacich, D. J., Ramadan, E., O'keefe, D. S., Bukhari, N., Wegorzewska, I., Ojeifo, O., Olszewski, R., Wrenn, C. C., Bzdega, T., Wroblewska, B., Heston, W. D., & Neale, J. H. (2002). Deletion of the glutamate carboxypeptidase II gene in mice reveals a second enzyme activity that hydrolyzes N-acetylaspartylglutamate. *Journal of Neurochemistry*, *83*, 20–29.

Cardinale, J., Martin, R., Remde, Y., Schafer, M., Hienzsch, A., Hubner, S., Zerges, A. M., Marx, H., Hesse, R., Weber, K., Smits, R., Hoepping, A., Muller, M., Neels, O. C., & Kopka, K. (2017a). Procedures for the GMP-compliant production and quality control of [(18)F]PSMA-1007: A next generation radiofluorinated tracer for the detection of prostate cancer. *Pharmaceuticals (Basel)*, 10.

Cardinale, J., Schafer, M., Benesova, M., Bauder-Wust, U., Leotta, K., Eder, M., Neels, O. C., Haberkorn, U., Giesel, F. L., & Kopka, K. (2017b). Preclinical evaluation of (18)F-PSMA-1007, a new prostate-specific membrane antigen ligand for prostate cancer imaging. *Journal of Nuclear Medicine*, *58*, 425–431.

Carter, R. E., Feldman, A. R., & Coyle, J. T. (1996). Prostate-specific membrane antigen is a hydrolase with substrate and pharmacologic characteristics of a neuropeptidase. *PNAS*, *93*, 749–753.

Croall, I., Smith, F. E., & Blamire, A. M. (2015). Magnetic resonance spectroscopy for traumatic brain injury. *Topics in Magnetic Resonance Imaging*, *24*, 267–274.

Guilarte, T. R., Mcglothan, J. L., Foss, C. A., Zhou, J., Heston, W. D., Kozikowski, A. P., & Pomper, M. G. (2005). Glutamate carboxypeptidase II levels in rodent brain using [125I]DCIT quantitative autoradiography. *Neuroscience Letters*, *387*, 141–144.

Maschauer, S., Haller, A., Riss, P. J., Kuwert, T., Prante, O., & Cumming, P. (2015). Specific binding of [(18)F]fluoroethyl-harmol to monoamine oxidase A in rat brain cryostat sections, and compartmental analysis of binding in living brain. *Journal of Neurochemistry*, *135*, 908–917.

Mesters, J. R., Barinka, C., Li, W., Tsukamoto, T., Majer, P., Slusher, B. S., Konvalinka, J., & Hilgenfeld, R. (2006). Structure of glutamate carboxypeptidase II, a drug target in neuronal damage and prostate cancer. *Embo Journal*, *25*, 1375–1384.

Pouwels, P. J., & Frahm, J. (1997). Differential distribution of NAA and NAAG in human brain as determined by quantitative localized proton MRS. *Nmr in Biomedicine*, *10*, 73–78.

Sacha, P., Zamecnik, J., Barinka, C., Hlouchova, K., Vicha, A., Mlcochova, P., Hilgert, I., Eckschlager, T., & Konvalinka, J. (2007). Expression of glutamate carboxypeptidase II in human brain. *Neuroscience*, *144*, 1361–1372.

Wroblewska, B., Wroblewski, J. T., Pshenichkin, S., Surin, A., Sullivan, S. E., & Neale, J. H. (1997). N-acetylaspartylglutamate selectively activates mGluR3 receptors in transfected cells. *Journal of Neurochemistry*, *69*, 174–181.

How to cite this article: Thomsen, M. B., Landau, A. M., Bender, D., & Cumming, P. (2023). Autoradiographic characterization of [^{18}F]PSMA-1007 binding in rat brain. *Synapse*, e22280. https://doi.org/10.1002/syn.22280